

The Origin of Infrared Emission from the Infrared Luminous Galaxy NGC 4418 *

Lei Shi and Qiu-Sheng Gu

Department of Astronomy, Nanjing University, Nanjing 210093; qsgu@nju.edu.cn

Received 2004 October 5; accepted 2005 January 7

Abstract We present a study of the origin of infrared (IR) emission in the optically normal, infrared luminous galaxy NGC 4418. By decomposing the stellar absorption features and continua in the range of 3600–8000 Å from the Sloan Digital Sky Survey into a set of simple stellar populations, we derive the stellar properties for the nuclear region of NGC 4418. We compare the observed infrared luminosity with the one derived from the starburst model, and find that star-forming activity contributes only 7% to the total IR emission, that as the IR emission region is spatially very compact, the most possible source for the greater part of the IR emission is a deeply embedded AGN, though an AGN component is found to be unnecessary for fitting the optical spectrum.

Key words: galaxies: general – galaxies: active – galaxies: stellar content – galaxies: individual (NGC 4418)

1 INTRODUCTION

One of the most important discoveries by the Infrared Astronomical Satellite (IRAS) was the discovery of a population of luminous infrared galaxies (LIRGs) with infrared luminosities above $10^{11}L_{\odot}$ (Soifer et al. 1984; Sanders & Mirabel 1996), that emit the bulk of the whole energy in the infrared band. As they are located at the bright end of the local luminosity function and have similar luminosities as quasars, hot debates have arisen on the nature of their energy source — starburst or/and AGN activity. Sanders et al. (1988) suggested that ultraluminous infrared galaxies with $L_{\text{IR}} > 10^{12}L_{\odot}$ may actually be dust-enshrouded quasars, and once the obscuring dust is swept away by radiation force and supernova explosions, the nuclear region will be cleared, then these objects will take on the appearance of optical quasars. On the other hand, many similarities have been found between ULIRGs and starburst galaxies (Joseph & Wright 1985; Rowan-Robinson & Crawford 1989; Condon et al. 1991), and Rigopolou et al. (1996) found that the starburst model can fit well the radio, infrared and soft X-ray observations of Sanders's

* Supported by the National Natural Science Foundation of China.

10 ULIRGs. Although it is now widely accepted that both star formation and AGN activity can power the LIRGs, the questions as to which of the two is dominant, and what connections there are between the two are still unclear. The mid-infrared (MIR) observation made by Genzel et al. (1998) showed that the majority of the ULIRGs in their sample are powered predominantly by young and hot stars rather than AGNs. However, many observations suggest that the frequency of AGNs occurring in LIRGs increases with their far-infrared (FIR) luminosity (Veilleux et al. 1995; Wu et al. 1998; Veilleux, Sanders & Kim 1999). It is interesting to note that a recent study of the spectral energy distributions (SED) of local ULIRGs has given a different result (Farrah et al. 2003): they found that starburst is dominant in 90% of the sample galaxies and that there is no clear trend for the fractional AGN luminosity to increase with the total luminosity.

NGC 4418 is a weakly barred, nearly edge-on Sa-type, infrared luminous galaxy with an IR luminosity nearly $10^{11} L_{\odot}$ (Sanders et al. 2003), which is probably interacting with a companion galaxy 24 kpc away (Evans et al. 2003). The optical spectrum does not show any clear AGN signature, and weak $H\alpha$ and absence of $H\beta$ emission suggest it is heavily obscured (Armus, Heckman & Miley 1989; Lehnert & Heckman 1995). Dudley & Wynn-Williams (1997) detected a very strong silicate grain absorption in the 8–13 μm spectrum, while no clear evidence exists for the predicted 18 μm absorption feature, this suggests that the infrared emission comes from an optically thick dust shell surrounding a compact power source, whose size is supposed to be less than a few parsecs. Dudley & Wynn-Williams proposed that a substantial portion of the infrared emission can be ascribed to a deeply dust-embedded AGN (see also Spoon et al. 2001). Other observational supports for AGN-dominated infrared emission include: (1) the warm infrared color ($f_{25\mu\text{m}}/f_{60\mu\text{m}} = 0.23$), similar to those of infrared galaxies that are believed to harbor an AGN (de Grijp et al. 1985); (2) a very compact core in infrared and radio ($< 0.5''$) (Condon et al. 1990; Evans et al. 2003); (3) a high HCN/HCO+ ratio, a large H_2 to $\text{Br}\gamma$ luminosity ratio and a large H_2 equivalent width (Imanishi et al. 2004). On the other hand, the following facts favor the starburst explanation: (1) the 3.3 μm polycyclic aromatic hydrocarbon (PAH) emission feature (Imanishi et al. 2004); (2) the CO absorption features detected by Ivanov et al. (2000); (3) the nuclear K-L color = 0.5 mag, typical for star-forming galaxies (Willner et al. 1984).

In this paper we use stellar population synthesis models to investigate the nature of the infrared emission of NGC 4418. The NGC 4418 spectrum is taken from the Sloan Digital Sky Survey (SDSS). We adopt $H_0 = 75 \text{ km s}^{-1} \text{ Mpc}^{-1}$, $\Omega_M = 0.3$ and $\Omega_{\Lambda} = 0.7$, so the SDSS fibre size of $3''$ corresponds to 390 pc.

2 STELLAR POPULATION SYNTHESIS

We use the same code as Cid Fernandes et al. (2004b). Here we give a brief presentation of the method. The code searches for a linear combination of 30 Simple Stellar Populations (30 SSPs for 3 different metallicities and 10 different ages) from the recent stellar population models of Bruzual & Charlot (2003). The match between the model and observed spectra is evaluated by the rule of minimum χ squared, and the search for the best parameters is carried out with a simulated annealing method, which consists of a series of 10^7 likelihood-guided Metropolis tours through the parameter space. We subtract the best matched model from the observed spectrum to derive a pure emission-line spectrum. Our code has also been successfully applied to a large sample of Seyfert 2 galaxies (Cid Fernandes et al. 2004b).

3 RESULTS

The spectrum of NGC 4418 was downloaded from SDSS DR2, and then corrected for Galactic extinction using the reddening law of Cardelli et al. (1989) and the A_B values listed in NED (Schlegel, Finkbeiner & Davis 1998) before starting the synthesis. It had also been rebinned to 1 Å bins and redshift corrected to the rest-frame. We normalize the SSP bases at $\lambda_0 = 4540$ Å, while for the observed spectra we use the median value between 4520 and 4570 Å. To represent a possible contribution of an AGN featureless continuum, we adopted an $F_\nu \propto \nu^{-1.5}$ power-law, which is typical for modeling Seyfert galaxies (Koski 1978). We choose the same 10 different-age SSPs as Tremonti (2003): $t = 5 \times 10^6$, 2.5×10^7 , 10^8 , 2.9×10^8 , 6.4×10^8 , 9×10^8 , 1.4×10^9 , 2.5×10^9 , 5×10^9 and 1.1×10^{10} yr, and three metallicities, $Z = 0.1, 0.2$ and $1Z_\odot$.

Figure 1 shows the spectral fitting result of NGC 4418. Shown are both the observed and synthetic spectra, as well as the “pure emission” ($F_\lambda^{\text{obs}} - F_\lambda^{\text{mod}}$) residual spectrum. The star formation history is shown in the right panel of the figure, with flux (x_j) and mass (μ_j) fractions for all 10 ages spanned by the base, plus the AGN power-law featureless continuum (FC) component.

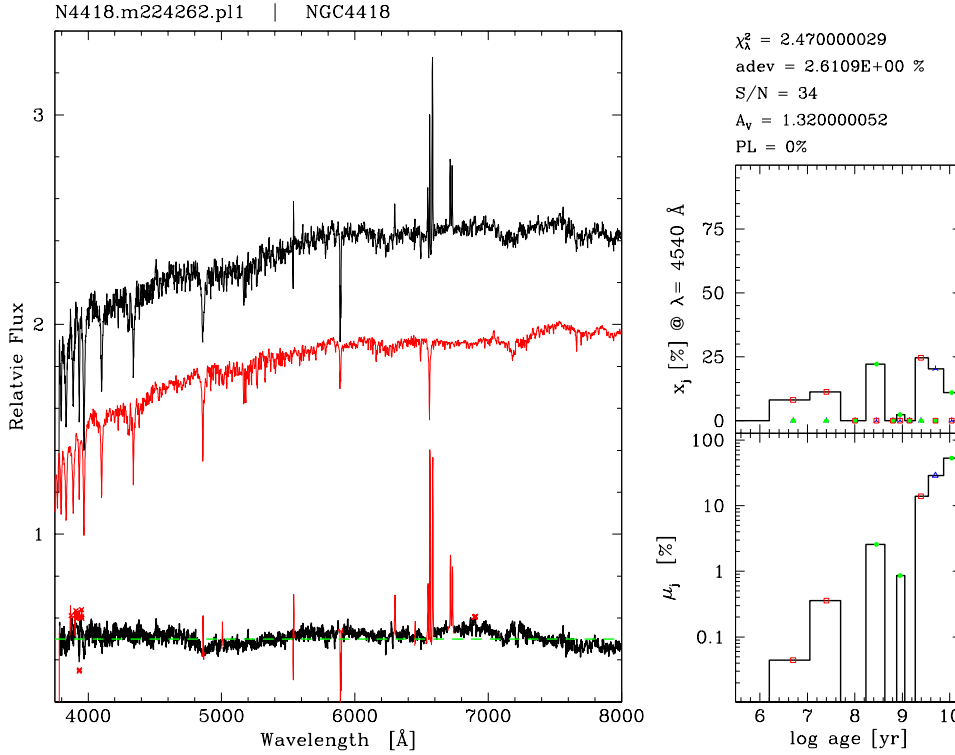


Fig. 1 Results of spectral fitting of NGC 4418. The left panel shows the observed, the synthetic and the residual ($F_\lambda^O - F_\lambda^M$) spectra, respectively. Spectral regions actually used in the synthesis are marked with a thick line, while masked regions, with a thin line. Crosses indicate points excluded from the synthesis by a 3 sigma clipping algorithm. Panels in the right show the population vector binned in the 10 ages of the base. The top panel corresponds to the population vector in flux fraction (x), normalized to $\lambda_0 = 4540$ Å, while the corresponding mass fractions vector (μ) is shown in the bottom. The power-law component x_{PL} is plotted with an arbitrary age of $10^{5.5}$ yr and marked by a diamond. No mass-fraction is associated to this component.

Table 1 lists the contributions to the stellar population from four components: an FC (x_{FC}) and three stellar components representing young ($t \leq 2.5 \times 10^7$ yr), intermediate ($2.5 \times 10^7 \leq t \leq 10^8$ yr) and old ($t \geq 2.5 \times 10^9$ yr) populations. The age definition is same as Cid Fernandes et al. (2004b). The parameters μ_Y , μ_I and μ_O are the mass fractions for the young, intermediate and old populations. Table 2 shows our results of emission lines (measured in the “pure” emission-line spectrum) and absorption lines (measured in the synthetic spectrum). For most of the stellar features we use the same indices as defined by Cid Fernandes et al. (2004a), which are based on the studies by Bica & Alloin (1986a, b) and Bica (1988) of star cluster and galaxy spectra. The measurements of the equivalent widths of CaII triplet lines are the same as used in Terlevich, Díaz & Terlevich (1990) and for $\text{H}\delta_A$ we adopt the definition of Worthey & Ottaviani (1997). For NGC 4418, it is the first time derivation of $\text{H}\beta$ and $[\text{OIII}]\lambda 5007$ luminosities. It is well known that we can distinguish narrow-line AGNs from normal star-forming galaxies by using flux ratios of emission lines, the so-called BPT diagrams (Baldwin, Phillips & Terlevich 1981; Veilleux & Osterbrock 1987). With our measurement of emission lines from the “pure” emission-line spectrum as shown in Table 2, we classify NGC 4418 as a LINER (see Fig. 2).

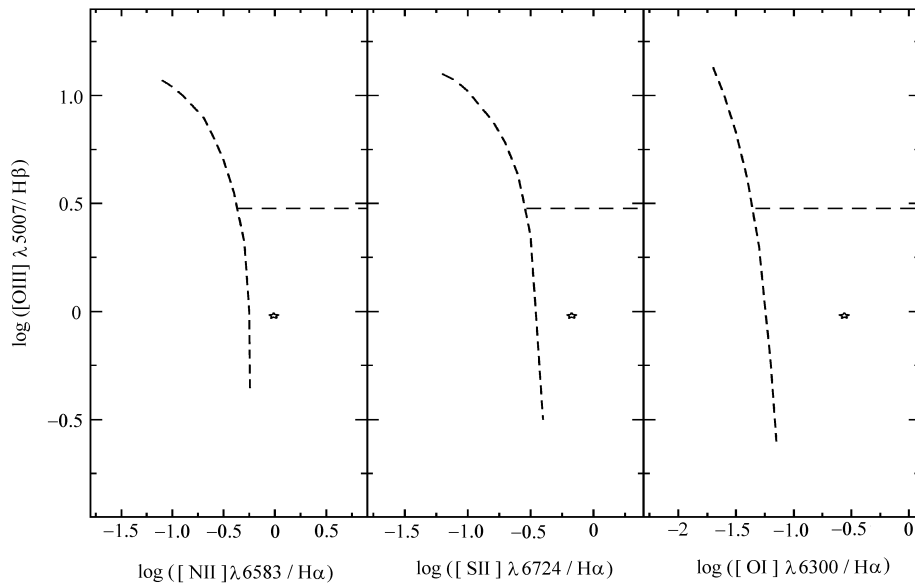


Fig. 2 Diagnostic diagrams. *left.* $\log([\text{NII}]\lambda 6583/\text{H}\alpha)$ vs. $\log([\text{OIII}]\lambda 5007/\text{H}\beta)$; *middle.* $\log([\text{SII}]\lambda 6724/\text{H}\alpha)$ vs. $\log([\text{OIII}]\lambda 5007/\text{H}\beta)$; *right.* $\log([\text{OI}]\lambda 6300/\text{H}\alpha)$ vs. $\log([\text{OIII}]\lambda 5007/\text{H}\beta)$. The short-dashed line divided NL AGNs from starburst galaxies is taken from Veilleux & Osterbrock (1987).

As we know, the optical continuum emission from AGN is mostly thermal emission from the accretion disk (Peterson 1997). For NGC 4418, Maiolino et al. (2003) found that it is a Compton-thick source, with a gaseous absorbing column density of $N_{\text{H}} > 10^{24} \text{cm}^{-2}$, which means that its central engine is completely obscured and makes no contribution to the optical continuum, this is also consistent with our stellar population synthesis results of $x_{\text{FC}} = 0.0$. Now, Monte Carlo simulations by Cid Fernandes et al. (2004b) have shown that typical 1σ uncertainty of x_{FC} is 2%, so the upper limit for the AGN contribution to the optical continuum is at most 2%.

Table 1 The Stellar Population Synthetic Results

Galaxy	x_{FC}	x_Y	x_I	x_O	μ_Y	μ_I	μ_O	A_V	χ^2_λ
(1)	(2)	(3)	(4)	(5)	(6)	(7)	(8)	(9)	(10)
NGC 4418	0	19.5	24.5	56.0	0.4	3.5	96.1	1.32	2.47

Columns 2–5: Population vector in the x_{FC} , x_Y , x_I , x_O description, in the percentage of the flux at 4540 Å. Columns 6–8: Percentage mass fractions associated to Y , I and O components. Column 9: Extinction (in V-band magnitude). Column 10: the χ^2 for the best matched fitting.

Table 2 Measurements of Absorption and Emission Lines in NGC 4418

Wavelength (Å)	Ion	Equivalent Width (Å)	Luminosity ^d
3933	Ca II K	6.03 ^b	–
4200	CN band	4.58 ^a	–
4300	G band	4.81 ^a	–
5173	Mg Ib	4.45 ^a	–
8498	Ca II	1.59 ^c	–
8542	Ca II	3.50 ^c	–
8662	Ca II	3.26 ^c	–
4861	H β	–	37.90
5007	[O III]	–	37.88
6300	[O I]	–	38.14
6548	[N II]	–	38.28
6563	H α	–	38.70
6583	[N II]	–	38.69
6716	[S II]	–	38.39
6730	[S II]	–	37.96

^a Equivalent width of stellar absorption features in Bica’s system.

^b $H\delta_A$ equivalent width defined by Worthey & Ottaviani (1997).

^c Equivalent width CaII triplet lines of Terlevich, Diaz & Terlevich (1990).

^d Luminosity in units of erg s⁻¹.

4 DISCUSSION

4.1 Stellar Population Properties

We have synthesized the whole spectrum of NGC 4418 and find that there is no contribution from the power law component, though it is commonly detected in Seyfert 2 nuclei (Cid Fernandes et al. 2004a). The young stellar population (5 Myr and 290 Myr) contributes nearly 20% of the flux at 4540 Å. As it has been shown that CaII triplet absorption lines around 8500 Å is a powerful diagnostic of star-forming activity (Terlevich et al. 1990), we measured the equivalent width of CaII triplet at $\lambda\lambda$ 8498, 8542, 8662 Å to be about 6.75 Å, a value similar to what is found in normal galaxies (Terlevich et al. 1990). Since the optical stellar features have

shown a substantial dilution, a possible reason to account for the high value of EW (CaII) is young star clusters with red supergiants (Terlevich et al. 1990). However, since the EW(MgIb) is also high, we adopted the same definition of the dilution factor as Terlevich et al. (1990), and found that the $D(\text{MgIb}) \approx 0.86$ and $D(\text{CaII}) \approx 0.95$. So, we could not completely eliminate the possibility of metal rich populations. A similar result has also been obtained from the $2.3\ \mu\text{m}$ CO observation of NGC 4418 by Ridgway, Wynn-Williams & Becklin (1994), who found the CO absorption feature and the slope of the continuum emission to be consistent with a late-type supergiant or metal-rich giant population.

Our synthetic results indicating a young stellar population are consistent with Evans et al. (2004), who found from a near-infrared color synthesized model, a 10–300 Myr starburst suffering a moderate level of visual extinction.

4.2 Nebular and Stellar Extinctions

Assuming Case B recombination and a standard reddening law, we could obtain the extinction for the emission nebulae from the observed $H\alpha/H\beta$ Balmer decrement (see Torres-Peimbert, Peimbert & Fierro 1989; Stasinska et al. 2004), and found it to be

$$A_V^{\text{nebular}} = 6.31 \times \log \left(\frac{F_{H\alpha}/F_{H\beta}}{I_{H\alpha}/I_{H\beta}} \right), \quad (1)$$

where $F_{H\alpha}/F_{H\beta}$ and $I_{H\alpha}/I_{H\beta}$ are the observed and intrinsic $H\alpha$ and $H\beta$ flux ratios, respectively. In this paper, we take the intrinsic ratio of $I_{H\alpha}/I_{H\beta}$ to be 2.86 (Osterbrock 1989).

For NGC 4418, the observed $F_{H\alpha}/F_{H\beta}$ (measured from the “pure” emission line spectrum) is equal to 6.42, hence the extinction for the emission nebulae is estimated to be $A_V^{\text{nebular}} = 2.22$ mag. As we have shown, our synthetic code also gives an estimate for the extinction of the stellar component, $A_V^{\text{stellar}} = 1.32$ mag. It is interesting to note that the nebular extinction A_V^{nebular} is 1.68 times A_V^{stellar} , this differential extinction between the nebular and stellar components is in very good quantitative agreement with the empirical studies (Calzetti, Kinney & Storchi-Bergmann 1994; Mas-Hasse & Kunth 1999) and the most recent study for a large number of SDSS galaxies by Cid Fernandes et al. (2004c).

4.3 Star Formation Rate

The stellar population synthetic code outputs the flux fractions of 30 stellar components for three different metallicities. By using Bruzual & Charlot (2003) theoretical model, we can estimate the total ionizing photons provided by those stellar components (see also Gu et al. 2004). For NGC 4418, we estimate a total of $Q(\text{H}^0) = 1.2 \times 10^{53}$ (s^{-1}) ionizing photons are available from all the 30 components. By using the relation between ionizing photons and star formation rate (SFR) given by Kennicutt (1998), we derive a star formation rate of $\text{SFR}_{\text{ion}} = 1.2 M_{\odot} \text{ yr}^{-1}$. Because the ionizing photons are directly deduced from the synthesized stellar population, without any need of correcting for extinction, the rate can be taken as an upper limit for the SFR a SDSS fiber size region.

We can also derive the SFR from the observed $H\alpha$ luminosity, which has been corrected for the nebular extinction and find $\text{SFR}_{\text{obs}} = 0.024 M_{\odot} \text{ yr}^{-1}$, which is much smaller than the theoretical prediction from ionizing photons and may indicate that the real star forming regions are even much more heavily obscured than what the observed Balmer decrement implies. The reason is that the aperture for the SDSS fiber is $3''$, but the infrared flux comes from an area within radius $< 0.5''$. We just used a very simple model for the extinction, but the real situation could be more complex. For our model, we cannot separate a modest extinction starburst with

a large area (such as $3''$) from a much heavier extinction nuclear starburst (such as $0.5''$) surrounded by a smaller extinction region. Both the difference in extinctions deduced from ionizing photons and observed $F_{H\alpha}/F_{H\beta}$ flux ratio and the compact IR emission morphology indicate that the case of NGC 4418 is much more complex than what we have assumed, and suggest that the extinction derived from the observed $F_{H\alpha}/F_{H\beta}$ flux ratio is severely underestimated. So, the SFR estimated from the observed $H\alpha$ luminosity is underestimated too. For the following discussion on the infrared emission, we will use the SFR deduced from theoretical ionizing photons which is less related with extinction and can be taken as the upper limit for SFR for the central $3''$ region.

4.4 Origin of Infrared Emission

It is well known that the infrared emission can be (1) emission associated with an active nucleus, either nonthermal flux coming directly from AGN or dust reradiation of nonthermal UV-optical continuum emission from the accretion disk; (2) emission by warm dust, warmed up in regions of star formation; (3) emission by cool dust heated by the general stellar radiation field (Rodríguez-Espinosa et al. 1987; Gu et al. 1996; Gonzalez Delgado et al. 2001). As we know, NGC 4418 is an IR luminous galaxy with $L_{\text{FIR}} = 10^{11} L_{\odot}$ (Sanders et al. 2003), but the optical appearance is rather normal. What is the origin for such an amount of infrared emission, and how much of the whole IR emission can be accounted for by the detected starburst?

According to the relation between SFR and far-IR emission obtained by Kennicutt (1998), the SFR deduced from total ionizing photons ($\text{SFR}_{\text{ion}} = 1.2 M_{\odot} \text{ yr}^{-1}$) is expected to produce a far-IR luminosity of $L_{\text{FIR}} = 2.7 \times 10^{43} \text{ erg s}^{-1}$, which can *only* account for 7% of the whole far-IR emission of NGC 4418 ($L_{\text{FIR}} = 3.86 \times 10^{44} \text{ erg s}^{-1}$). We notice that NGC 4418 is an Sa galaxy, and that the IR and radio observations suggest that the IR emission from NGC 4418 is spatially very compact ($< 0.5 \text{ arcsec}$) (Dudley & Wynn-Williams 1997; Evans et al. 2003), so the central energy source must be very compact, too, either an obscured nuclear starburst or a hidden AGN. Since the SDSS fiber size is much larger (3 arcsec), it should cover a much larger area than the region of infrared emission. Thus the SDSS fiber size covering factor is not the main cause for such a small predicted-to-observed far-infrared emission ratio.

As either a deeply imbedded AGN or a heavily obscured nuclear starburst, or maybe both, can account for the excess of far-infrared luminosity in NGC 4418, we cannot distinguish them only by our simple model and the SDSS optical spectrum. However, we can use the available multi-wavelength data of NGC 4418 for our further understanding, especially the infrared observations which are not so sensitive to extinction. Recently, Imanishi et al. (2004) presented near-infrared and millimeter observations of the nucleus of NGC 4418, they detected a $3.3 \mu\text{m}$ PAH emission luminosity of $7 \times 10^{39} \text{ erg s}^{-1}$ from the central $\sim 2 \text{ arcsec}^2$ region. As the PAH emission is widely believed to originate in stellar activity, a corresponding $\text{SFR}_{\text{PAH}} = 0.297 M_{\odot} \text{ yr}^{-1}$ was derived for the central $\sim 2 \text{ arcsec}^2$ region. Because the SDSS fiber covers a much larger area than this region, $\text{SFR}_{\text{obs}} < \text{SFR}_{\text{PAH}} < \text{SFR}_{\text{ion}}$ is also consistent with our results, so the case of very heavily obscured nuclear starburst is less possible. The only possible origin for the huge far-IR luminosity in NGC 4418 is a deeply buried AGN, this is also supported by the observed high values of the $\text{HCN}/\text{HCO}+$ and H_2 emission line luminosity ratios, the large H_2 to $\text{Br}\gamma$ ratio and the $\text{EW}(\text{H}_2)$ (Imanishi et al. 2004).

5 CONCLUSIONS

We have reproduced the spectrum of NGC 4418 from 3600 to 8000 \AA with theoretical stellar population synthesis. The synthetic results and the observed equivalent width of the Ca II triplets indicate a moderately-obscured starburst activity. We find that, in terms of energy, it

is not significant to account for the huge IR emission in NGC 4418, which is consistent with the recent near-IR observation by Imanishi et al. (2004). Combined with other observations, we argue that the central power source of NGC 4418 is most likely a composition of a young compact starburst with a relative small contribution to the total infrared luminosity and a deeply embedded AGN as the dominant power source.

Acknowledgements We are grateful to the referees, Jiasheng Huang and Jorge Melnick, for constructive comments. This work is supported by the National Natural Science Foundation of China, under grants 10103001 and 10221001, and the National Key Basic Research Science Foundation (NKBRSG 19990754). Funding for the creation and distribution of the SDSS Archive has been provided by the Alfred P. Sloan Foundation, the Participating Institutions, the National Aeronautics and Space Administration, the National Science Foundation, the U.S. Department of Energy, the Japanese Monbukagakusho, and the Max Planck Society. The SDSS web site is <http://www.sdss.org/>. SDSS is managed by the Astrophysical Research Consortium (ARC) for the Participating Institutions. The Participating Institutions are the University of Chicago, Fermilab, the Institute for Advanced Study, the Japan Participation Group, the Johns Hopkins University, Los Alamos National Laboratory, the Max-Planck-Institute for Astronomy (MPIA), the Max-Planck-Institute for Astrophysics (MPA), New Mexico State University, University of Pittsburgh, Princeton University, the United States Naval Observatory, and the University of Washington. SC thanks the Alexander von Humboldt Foundation, the Federal Ministry of Education and Research, and the Programme for Investment in the Future (ZIP) of the German Government for financial support. JB acknowledges the receipt of ESA post-doctoral fellowship.

References

- Armus L., Heckman T. M., Miley G. K., 1989, *ApJ*, 347, 727
Baldwin J. A., Philips M. M., Terlevich R., 1981, *PASP*, 93, 5
Bica E., Alloin D., 1986a, *A&A*, 162, 21
Bica E., Alloin D., 1986b, *A&A*, 166, 83
Bica E., 1988, *A&A*, 195, 76
Bruzual G., Charlot S., 2003, *MNRAS*, 344, 1000
Calzetti D., Kinney A. L., Storchi-Bergmann T., 1994, *ApJ*, 429, 582
Cardelli J. A., Storchi-Bergmann T., Schmitt H. R., 1989, *MNRAS*, 297, 579
Cid Fernandes R., Delgado R. M. G., Schmitt H. et al., 2004a, *ApJ*, 605, 105
Cid Fernandes R., Gu Q., Melnick J. et al., 2004b, *MNRAS*, 355, 273
Cid Fernandes R., et al. 2004c, *MNRAS*, in press
Condon J. J., Helou G., Sanders D. B. et al., 1990, *ApJS*, 73, 359
Condon J. J., Huang Z.-P., Yin Q. F. Thuan T. X., 1991, *ApJ*, 378, 65
de Grijp M. H. K., Miley G. K., Lub J. et al., 1985, *Nature*, 314, 240
Dudley C. C., Wynn-Williams C. G., 1997, *ApJ*, 488, 720
Evans A. S., Becklin E. E., Scoville N. Z. et al., 2003, *AJ*, 125, 2341E
Farrah D., Afonso J., Efsthathiou A. et al., 2003, *MNRAS*, 343, 585
Genzel R., et al, 1998, *ApJ*, 498, 579
Gonzalez Delgado R., Heckman T., Leitherer C., 2001, *ApJ*, 546, 845
Gu Q., Huang J. H., Su H. J. et al., 1997, *A&A*, 319, 92
Gu Q., Cid Fernandes R., Melnick J. et al, 2004, *MNRAS*, submitted
Imanishi M., Nakanishi K., Kuno N. et al., 2004, *AJ*, 128, 2037
Ivanov V. D., Rieke G. H., Groppi C. E. et al., 2000, *ApJ*, 545, 190

- Joseph R. D., Wright G.S., 1985, MNRAS, 214, 87
Kennicutt R. C. Jr., 1998, ARA&A, 36, 189
Kewley L.J., et al. 2000, ApJ, 530, 704
Koski A. T., 1978, ApJ, 223, 56
Lehnert M. D., Heckman T. M., 1995, ApJS, 97, 89
Maiolino R., Comastri A., Gilli R. et al., 2003, MNRAS, 344, L59
Mas-Hesse J. M., Kunth D., 1999, A&A, 349, 765
Osterbrock D. E., 1989, *Astrophysics of Gaseous Nebulae and Active Galactic Nuclei* (Mill Valley: University Science Books)
Peterson B. M., 1997, *An Introduction to Active Galactic Nuclei* Cambridge: Cambridge Univ. Press
Ridgway S. E., Wynn-Williams C. G., Becklin E. E., 1994, ApJ, 428, 609
Rigopoulou D., Lawrence A., Rowan-Robinson M., 1996, MNRAS, 278, 1049
Roche P. F., Aitken D. K., Smith C. H. et al., 1986, MNRAS, 218, 19
Rodriguez-Espinosa J. M., Rudy R. J., Jones B., 1987, ApJ, 312, 555
Roussel H., Helou G., Beck R. et al., 2003, ApJ, 593, 733
Rowan-Robinson M., Crawford J., 1989, MNRAS, 238, 523
Sanders D. B., Mazzarella J. M., Kim D. C. et al., 2003, AJ, 126, 1607
Sanders D. B., Mirabel I. F., 1996, ARA&A, 34, 749
Sanders D. B., Soifer B. T., Elias J. H. et al., 1988, ApJ, 325, 74
Schlegel D. J., Finkbeiner D. P., Davis M., 1998, ApJ, 520, 525
Soifer B. T. et al, 1984, ApJ, 283, L1
Spoon H. W. W., Keane J. V., Tielens A. G. G. M. et al., 2001, A&A, 365, L353
Stasinska G., Mateus A. Jr., Sodré L. Jr. et al., 2004, A&A, 420, 475
Terlevich E., Díaz A.I., Terlevich R., 1990, MNRAS, 242, 271
Torres-Peimbert S., Peimbert M., Fierro J., 1989, ApJ, 345, 186
Tremonti C., 2003, PhD thesis, Johns Hopkins University
Vacca W., Conti P., 1992, ApJ, 401, 543
Veilleux S., Osterbrock D. E., 1987, ApJS, 63, 295
Veilleux S., Kim D. C., Sanders D. B. et al., 1995, ApJS, 98, 171
Veilleux S., Sanders D. B., Kim D. C., 1999, ApJ, 522, 139
Willner S. P., Ward M., Longmore A. et al., 1984, PASP, 96, 143
Worthey G., Ottaviani D. L., 1997, ApJS, 111, 377
Wu H., Zou Z. L., Xia X. Y. et al., 1998, A&AS, 132, 181
Yun M. S., Reddy N. A., Condon J. J., 2001, ApJ, 554, 803